PNAS RESEARCH ARTICLE | NEUROSCIENCE

Association neurons in the crow telencephalon link visual signs to numerical values

Maximilian E. Kirschhock[a] and Andreas Nieder[a,1]

Edited by Ranulfo Romo, El Colegio Nacional, Mexico City, Mexico; received August 12, 2023; accepted September 20, 2023

Many animals can associate signs with numerical values and use these signs in a goal-directed way during task performance. However, the neuronal basis of this semantic association has only rarely been investigated, and so far only in primates. How mechanisms of number associations are implemented in the distinctly evolved brains of other animal taxa such as birds is currently unknown. Here, we explored this semantic number-sign mapping by recording single-neuron activity in the crows' nidopallium caudolaterale (NCL), a brain structure critically involved in avian numerical cognition. Crows were trained to associate visual shapes with varying numbers of items in a number production task. The responses of many NCL neurons during stimulus presentation reflected the numerical values associated with visual shapes in a behaviorally relevant way. Consistent with the crow's better behavioral performance with signs, neuronal representations of numerical values extracted from shapes were more selective compared to those from dot arrays. The existence of number association neurons in crows points to a phylogenetic preadaptation of the brains of cognitively advanced vertebrates to link visual shapes with numerical meaning.

numbers | corvid songbird | associations | *Corvus* | semiotics

Significance

The association between numbers and signs constitutes a presymbolic semantic mapping process. We explored the neurobiological underpinnings of semantic number associations in a bird species that lacks the mammalian-specific cerebral cortex. We recorded single neurons in a telencephalic associative brain region of crows trained to associate the numerical values of dot displays with visual signs to solve a number task. The responses of neurons reflected the numerical values associated with visual signs in a behaviorally relevant way. Consistent with the crows' better behavioral performance with signs, neuronal representations of numerical values extracted from signs were more selective compared to those from dot arrays. Number association neurons in crows point to a phylogenetic preadaptation for presymbolic semantic mapping.

Different animal species across the animal kingdom assess numerical quantity and use this information to their survival advantage (1). The capacity for numerical competence is shared with humans through a nonsymbolic, evolutionarily primordial system (2), the approximate number system (ANS), which is thought to form a basis for human-specific symbolic number representations (3, 4). This system enables perceptual-like and approximate estimation of numerical quantity. As key characteristics, the ANS gives rise to numerical distance effects (numerical distant quantities are more easily discriminated) and numerical size effects (at a given numerical distance, smaller quantities are more easily discriminated) (1).

Building on the faculty for symbolic understanding, humans learn to deal with number symbols from an early age, ultimately allowing them to precisely determine cardinality and perform complex arithmetic (5–7). Before signs, such as the Arabic numerals, become symbolic representations of numerical quantity, an association between the numerical value and an arbitrary sign must be formed in long-term memory to give rise to indexical number representations (5, 8). Indexical number-sign associations can also be grasped by animals from various taxa, such as nonhuman primates (9–17), a parrot and pigeons (18–21), and bees (22). As indications of the semantic mapping, the characteristics of approximate number representations become imprinted onto visual signs. This leads to ANS-typical numerical distance and size effects with these signs (12), as well as Stroop-like effects in trials in which set size and number signs provide contradictory magnitude information (23). Such semantic associations between numerical values and arbitrary signs provide behavioral advantages as they improve deliberate decision-making in animals (24, 25) and three-year-old children (26).

The neuronal basis of semantic associations has only been investigated in the brains of primates so far. The prefrontal cortex (PFC) possesses a large proportion of association neurons that link numerical values to visual shapes in a behaviorally relevant way (27). However, the numerical aptitude of vertebrates that do not possess a layered neocortex suggests that semantic numerical associations can also be realized by differently evolved brain structures. This begs the question of whether similar or different mechanisms of number associations are implemented in the brains of different vertebrate taxa. The avian telencephalon shows striking anatomical differences compared to mammals that are indicative of an independent trajectory of brain evolution (28–30). Yet, birds such as crows show elaborate numerical abilities (31–33). Within the crow pallial telencephalon, the nidopallium caudolaterale (NCL) is ideally situated to facilitate semantic associations: First, it constitutes the key hub of number processing in the avian brain (32–38). Second, it operates at the apex of the telencephalic hierarchy, receives afferent information from

Author affiliations: [a]Animal Physiology Unit, Institute of Neurobiology, University of Tübingen, Tübingen 72076, Germany

Author contributions: M.E.K. and A.N. designed research; performed research; analyzed data; and wrote the paper.

The authors declare no competing interest.

This article is a PNAS Direct Submission.

[1]To whom correspondence may be addressed. Email: andreas.nieder@uni-tuebingen.de.

Published October 30, 2023.

all sensory modalities and outputs information to premotor structures (39, 40). Third, it plays a crucial role in learning and memory processes (41–44). Last, it upholds representations of associations between pairs of arbitrary stimuli (45–48). We therefore hypothesized that the numerical abilities of crows emerging from the pallial endbrain could also give rise to association neurons that map numerical meaning onto arbitrary visual shapes. Here, we recorded single-neuron activity from the NCL of crows trained to associate the numerical values of dot displays with numeral signs to solve a number production task.

Results

We trained two carrion crows (*Corvus corone*) to judge the numerical value of instruction stimuli and to subsequently produce the instructed number via pecking responses to a touch-sensitive monitor (49) (Fig. 1*A*). Stimuli instructing the numbers 1 to 5 were presented in two protocols (Fig. 1*B*), a "dot protocol" and a "sign protocol". During training, the crows had learned that each of the Arabic numeral signs was associated with a specific numerical value. Both stimulus protocols were shown in two conditions (standard and control conditions; Fig. 1*B*) to prevent crows from discriminating covarying non-numerical visual features and to promote generalization across sign appearance. The temporal arrangement of the motor execution period was controlled in such a way that crows could only rely on the absolute number of self-generated actions and not on alternative timing strategies to solve the task. These controls have been described in detail before (33).

Number Production Performance. The crows were highly proficient on the task (crow 1: 74.7 ± 5.1%, 71 sessions; crow 2: 72.1 ± 4.0%, 56 sessions; mean ± SD). Fig. 1 *C* and *D* shows the average performance of each crow over all recording sessions, separately for the dot and the sign protocol. Generally, accuracy varied as a function of instructed number, with larger numbers less accurately produced. Number 3 as the middle of the tested number range is an exemption to this general trend. Further, both crows were more accurate on sign trials compared to dot trials of the same number. However, performance for all instructed numbers in both stimulus protocols were highly above the respective chance level (solid black lines in Fig. 1 *C* and *D*; instruction number 1: 33.3%; 2: 25%; 3: 20%; 4: 16.7%; 5: 14.3%; see ref. 33 for details). The crows' number production behavior exhibits numerical distance and size effects, indicating that dots and signs were represented as numerical quantities (33).

Neuronal Responses in the NCL. We recorded the activity of 339 single neurons in the telencephalic nidopallium caudolaterale, NCL, of both crows while they performed the task. We have shown previously that neurons in the NCL translate the instructed number into a motor plan for the upcoming number of pecks during the motor planning period (33). Here, we focused on the sensory stimulus presentation period prior to motor planning (Fig. 1*A*). To identify neurons selective to the numerical values of dot arrays and signs, we performed two-factorial sliding-window ANOVAs with factors "instruction number" (1 to 5) and "stimulus protocol" (dots or signs) on the neurons' firing rates (see *Methods* for detailed description). For further analyses on associative neurons, we selected all neurons with a main effect for instruction number, including number-selective neurons with an additional main effect for stimulus protocol. We found that half of all recorded neurons (170/339, 50.2%) had significant intervals of selectivity for number during the presentation of the instruction stimulus. Number-selective neurons fired maximally to one of the presented instruction numbers during their respective selective intervals. Fig. 2 shows two exemplary number-selective

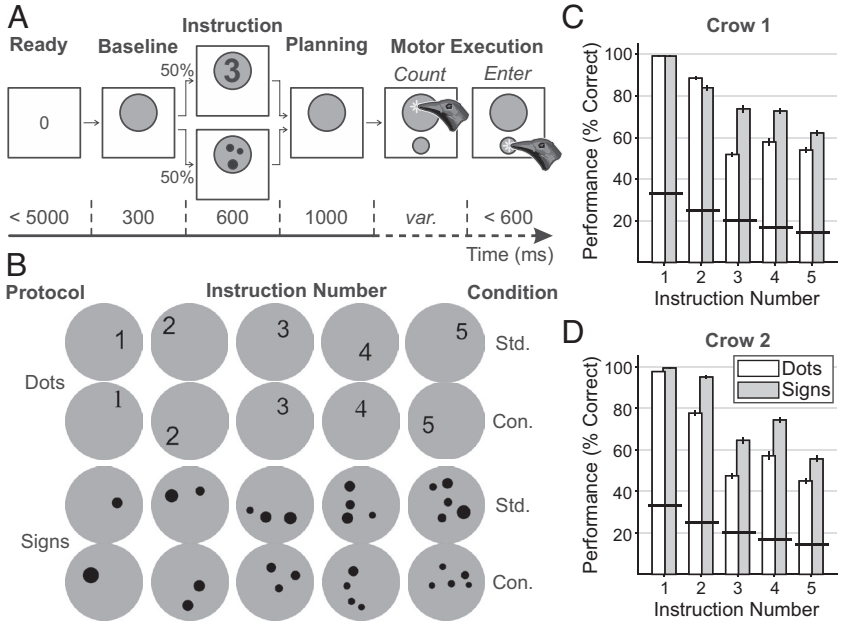

Fig. 1. Number production task and performance. (*A*) Number production task. A trial was initiated by the crow positioning its head in front of the touch-sensitive monitor. An instruction stimulus appeared cueing the crow for 1 to 5 pecking responses (three pecks cued in the example shown), in half of the trials either by a random dot display or Arabic numerals, respectively. Following, the crow planned the upcoming number of pecks during a brief motor planning period. During the subsequent motor execution period, the crow was prompted to peck the instructed number of times. There were systematically varied pauses between pecking actions to prevent the crow from using alternative timing strategies to solve the task (not shown). Finally, the crow indicated reaching the target number by pecking at the enter key. (*B*) Example instruction stimuli. Each instruction number 1 to 5 was indicated by two stimulus protocols, dot arrays, and signs (Arabic numerals). Standard and control stimuli controlled for non-numerical factors in the dot numerosities (position, size, density, and total dot area), and shape appearance (different font types) of the signs, respectively. (*C*) Average task performance (% correct) of crow 1 (71 sessions). Performance is shown for all instruction numbers, separately for the two stimulus protocols, dots (white bars) and signs (gray signs). Error bars show the SEM over session. Black horizontal lines in the graphs denote the chance level for each instruction number. (*D*) Average task performance of crow 2 (56 sessions). Same as in *C*.

neurons that fire maximally for numerical value 1 (Fig. 2 *A*–*E*) or 5 (Fig. 2 *F*–*J*), irrespective of whether dots or signs signaled the instructed number. The neuron in Fig. 2*A* fired the most both when one dot was presented and when the Arabic numeral "1" was shown (Fig. 2*B*). This neuron also responded similarly across protocols to the presentation of other instruction numbers. This became evident in the neuron's tuning curve (Fig. 2*C*) calculated over its interval of selectivity (gray shaded area in Fig. 2 *A* and *B*). The tuning curves were largely overlapping for both stimulus protocols. Similarly, the second example neuron responded equally strong to its preferred instruction number 5 irrespective of the stimulus protocol, i.e., five dots (Fig. 2*F*) or Arabic numeral "5" (Fig. 2*G*). The tuning functions (Fig. 2*H*) of this neuron were also largely superimposed across stimulus protocols.

Neuronal Associations of Signs with Numerical Values. Such number-selective neurons in the NCL may constitute a candidate substrate for the neuronal association of numerical values between numerosity in dot displays and arbitrary visual signs associated with numerical values. If so, these neurons are expected to exhibit very similar tuning functions to the instructed numbers irrespective of the protocol of the instructing stimulus. To test this, we performed a time-resolved correlation analysis of individual cell's tuning functions between dot and sign protocols. For all 170 number-selective neurons, we calculated cross-correlation coefficients (CCs) in a sliding-window manner to the real data and to shuffled data. A CC of 0 indicates no correlation, whereas a CC of 1 signals perfect correlation. To assess the significance of the correlation, we derived receiver operating characteristics (ROC) at every point in time between real CCs and CCs based on shuffled data to control for chance occurrence (shuffled predictors, SPs). The area under the ROC (AUROC) value expresses the degree of similarity of a neuron's tuning functions for dot and sign protocols (see *Methods* for details), with a value of 0.5 indicating chance similarity and a value of 1 signaling perfect similarity.

Using this approach, we find that the tuning curves of 133 NCL neurons (39.2% of the population of 339 cells; 78.2% of 170 number-selective neurons) were significantly correlated during stimulus presentation in the dot and sign protocols; such neurons were thus characterized as "number association neurons". For example, the neurons in Fig. 2 constituted such association neurons: Shortly after the onset of the instruction stimulus, the

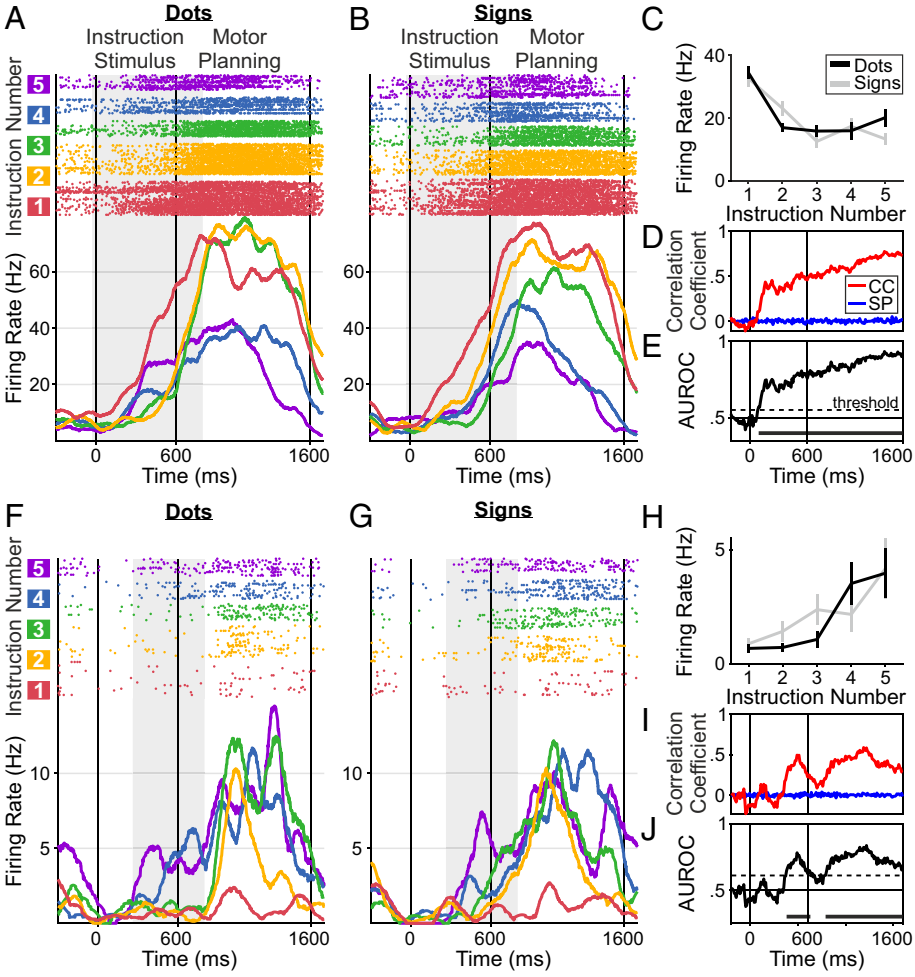

Fig. 2. Exemplary number-selective neurons in the NCL. (*A*–*E*) Example neuron preferring instruction number 1. Neuronal activity separately for dot protocol (*A* and *F*) and sign protocol (*B* and *G*) is displayed as dot raster histograms (*Top*; each dot representing one action potential) and spike-density functions (*Bottom*; smoothed with a 150-ms Gaussian kernel) in the *Bottom*. Responses to specific instruction numbers are color-coded (legend right of raster plots) and aligned to onset of the instruction stimulus (0 ms). (*C*) Average tuning curves (to the dot and sign protocol) of the neuron during its selective interval (indicated by the shaded area in the histograms, determined by sliding window ANOVA, see *Methods*). (*D*) Cross-correlation coefficients (CC) and SP values of the respective neurons over duration of the trial. Same alignment as for the histograms. (*E*) AUROC values as a function of trial time for the respective neurons. Same alignment as in the histograms. The horizontal black line at 0.5 shows chance level AUROC, the dashed line indicates the significance threshold, and the solid, thick lines indicate periods of significant association (see *Methods* for details). (*F*–*J*) Example neuron preferring instruction number 5. (*F* and *G*) Detailed neuronal responses of this neuron to dots and signs, respectively. Same layout as *A* and *B*. (*H*) Average tuning curves of this neuron. Same layout as in *C*. (*I*) Cross-correlation coefficients (CC) and SP values of the respective neuron. Same layout as in *D*. (*J*) AUROC values for this respective neuron. Same layout as in *E*.

correlation coefficients of both cells increased from 0 during the prestimulus period to values of around 0.5 during instruction stimulus presentation (Fig. 2 *D* and *I*). While the first example neuron preferring number 1 showed early and consistently high correlation indicating sustained association (Fig. 2*D*), the second example neuron preferring number 5 associated numerical values only later in the stimulus presentation period (Fig. 2*I*). For both neurons, significant association activity was captured by the significant AUROC values over the course of a trial (Fig. 2 *E* and *J*).

We found that the number of significantly associating neurons increased with the continued duration of the instruction period (Fig. 3*A*). The black bars in the lower part of Fig. 3*A* indicate time-bins with significant AUROC values for each association neuron (same as in Fig. 2 *E* and *J*). Since many of these neurons associated the numerical value of the dot display and the linked sign during more than one time point (individual traces in the bottom part of Fig. 3*A*), the entire instruction period is covered by the population of association neurons (bar height in the top part of Fig. 3*A*).

Behavioral Relevance of Neuronal Associations. We tested whether the activity of association neurons correlated with the behavioral outcome in a trial. We hypothesized that if association neurons failed to link dot numerosity with the respective sign, the crows would be prone to produce erroneous numbers of actions. To test this prediction, we calculated CCs in the instruction stimulus period for correctly performed trials and compared them to error trials in which the crows were producing an incorrect number of pecks. Since both crows made almost no errors for number 1 trials, the CCs were calculated only for a subset of instruction numbers, e.g., instruction numbers 2 to 5, matched for tuning curves in both stimulus protocols. For all 133 association neurons, we compared CCs for correct and error dot and sign trials. As visible in Fig. 3*B*, the systematic pattern of CCs apparent for correct trial associations (*Top*), was absent during error trials (*Bottom*), indicating that association neurons failed to associate dots and signs in their respective significance interval. As a consequence, the average population CCs were significantly reduced in error trials compared to correct trials (Fig. 3*C*; CCs(correct) vs. CC(error) during the first half stimulus period, $P < 0.05$, $n = 133$ neurons, Wilcoxon signed-rank test), especially during the second half of the instruction period ($P < 0.001$). As a control, no difference was detected between CCs of correct and error trials during the baseline period prior to stimulus presentation ($P = 0.7$). This suggests that the neurons' failure to properly associate the numerical value from dot displays with visual signs contributed to errors. Association neurons were thus of significance to the behavioral performance of the crows.

Numerical Tuning of Association Neurons. We next investigated the numerical tuning properties of association neurons in the two stimulus protocols. To this end, we first determined every association neuron's preferred numerosity of dots and Arabic numeral during their ANOVA-selective intervals. With a slight overrepresentation of number 1, all five instruction numbers were represented as preferred numbers by the association neurons in dot (Fig. 4*A*) and sign protocol (Fig. 4*B*). Population tuning functions were constructed from normalized tuning curves of all neurons preferring a certain instruction number. In the dot protocol, the tuning curves showed a numerical distance effect, i.e., neuronal activity gradually decreased for nonpreferred numerosities more remote from the preferred numerosity (Fig. 4*C*). In addition, the tuning curves in the dot protocol showed a numerical size effect by increasing tuning width as a function of the increasing value of the preferred numerosity, rendering larger numbers less precisely represented than smaller numbers (Fig. 4*C*). Neither distance

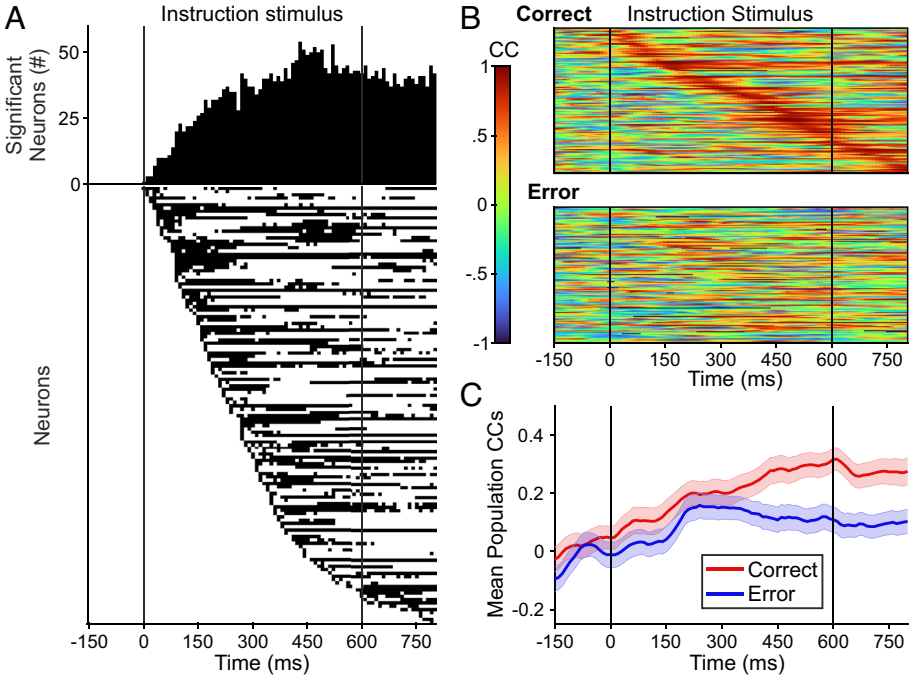

Fig. 3. Association neurons in the NCL. (*A*) Frequency and time course of all association neurons in the NCL ($n = 133$). Number of significant (as determined by correlation analysis) association neurons as a function of time during the instruction stimulus period (vertical lines indicate onset and offset of physical stimulus) in the *Top*, for each neuron individually in the *Bottom*. Each line is one neuron; each black pixel shows a time-bin with a significant AUROC value. Neurons are sorted by the latency of the first significant time-bin. (*B*) Temporal profile of association neurons during correct (*Upper*) and error trials (*Lower*). Same presentation as in the bottom part of *A*, with correlation coefficients (CC) color-coded. Individual neurons' CCs are smoothed over time (running mean, window size 5 time-bins, see *Methods*) and sorted by time point of maximal CC during stimulus presentation of correct trials. (*C*) Mean population CCs over time. Mean overall ($n = 133$) association neurons' CCs for correct (red) and error trials (blue). Shaded error bars indicate the SEM.

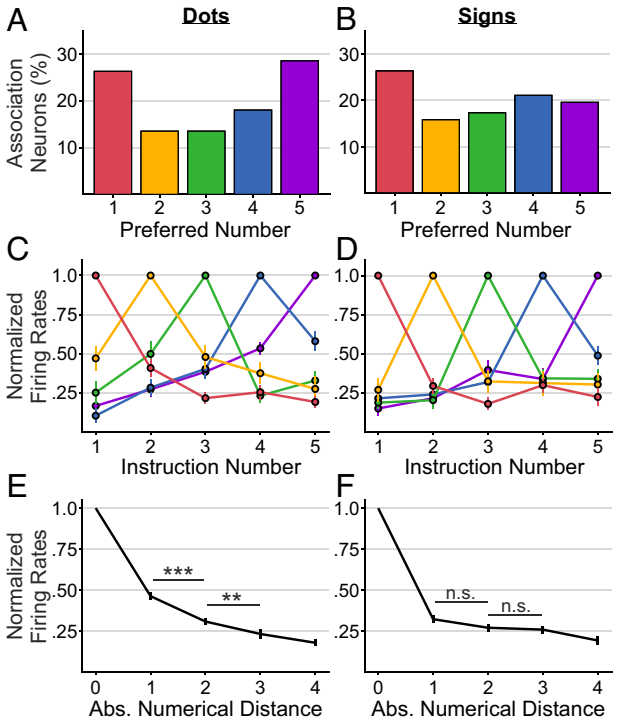

Fig. 4. Numerical tuning properties of association neurons. (*A* and *B*) Relative frequency of preferred instruction numbers of all ($n = 133$) association neurons for the dot (*A*) and the sign protocol (*B*). (*C* and *D*) Average tuning functions of all association neurons preferring each instruction number (color-coded) in the respective stimulus protocol (*C*, dots; *D*, signs). Lines and symbols show the mean, error bars the SEM over units. (*E* and *F*) Average tuning curve as a function of absolute numerical distance (*Methods*) for dot (*E*) and sign protocol (*F*). Error bars show the SEM, asterisks depict the significance (*$P < 0.05$; **$P < 0.01$; ***$P < 0.001$; *n.s.*: not significant).

nor size effects were evident for the categorical tuning function in the sign protocol in which the preferred numerosity elicited the strongest responds, but all nonpreferred numerosities elicited similarly low firing rates (Fig. 4*D*). We quantified this difference by plotting the average population tuning curves as a function of numerical distance. The numerical distance effect predicts a gradual decay of activity for nonpreferred numerosities as a function of distance from the preferred numerosity. For the dot protocol, we found significantly decreased activity for the second compared to the first absolute numerical distance on the tuning function, and for the third compared to the second absolute numerical distance (Num. dist. 1 vs. 2: $P < 0.001$; 2 vs. 3: $P < 0.01$; pair-wise Wilcoxon signed-rank tests) (Fig. 4*E*). In contrast, such differences were absent for the sign protocol (Fig. 4*F*) (1 vs. 2: $P = 0.06$; 2 vs. 3: $P = 0.82$). Together, this demonstrates a more precise neuronal representation of numerical values from Arabic numerals that was consistent with better performance of the crows in the sign protocol compared to the dot protocol (Fig. 1 *C* and *D*).

Time Course of Cross-Protocol Population Decoding. Last, we examined the temporal dynamics of the numerical information being extracted by the entire sampled NCL population, irrespective of number selectivity. For this, we used a time-resolved population decoding approach based on support vector machine (SVM) classifiers. In brief, within sliding time windows throughout the trial, we trained SVM models on instruction numbers and respective firing rates of the entire population of neurons with a sufficient number of trial repetitions ($n = 270$ neurons; see *Methods* for details). These firing rates came from trials of either the dot or the sign protocol. Within the same time windows, trained models were then tested to predict the instruction number of previously unseen trials, either from the same stimulus protocol as used for training (two within-protocol conditions) or from the respective other protocol (two across-protocol transfer). By comparing actual instruction numbers with the predicted ones, we derived the time-courses of classifier accuracies for each of the four specific conditions (Fig. 5*A*).

All specific conditions were significantly decodable by the population within the period of stimulus presentation. As expected, the within-protocol condition (i.e., training on dots and testing on dots and training on signs and testing on signs) reached the highest accuracy levels of up to 80% and 50% for the sign-to-sign and dot-to-dot condition, respectively (Fig. 5*A*). The onset of significant decoding was reached soon after instruction stimulus onset (first significant decoding indicated by downward-pointing triangles on the x-axis of Fig. 5*A*) with short latencies ($latency_{dot\text{-}dot}$ = 100 ms from stimulus onset, $latency_{sign\text{-}sign}$ = 40 ms; note, however, that these latencies are smeared out along the time-axis due to the size of the sliding window, see *Methods* for details).

As anticipated, the accuracy of cross-protocol transfer reached considerably smaller values of around 30% accuracy. Still, we found that this decoding accuracy was significantly above chance for sign-to-dot and dot-to-sign transfers (Fig. 5*A*). The onset of

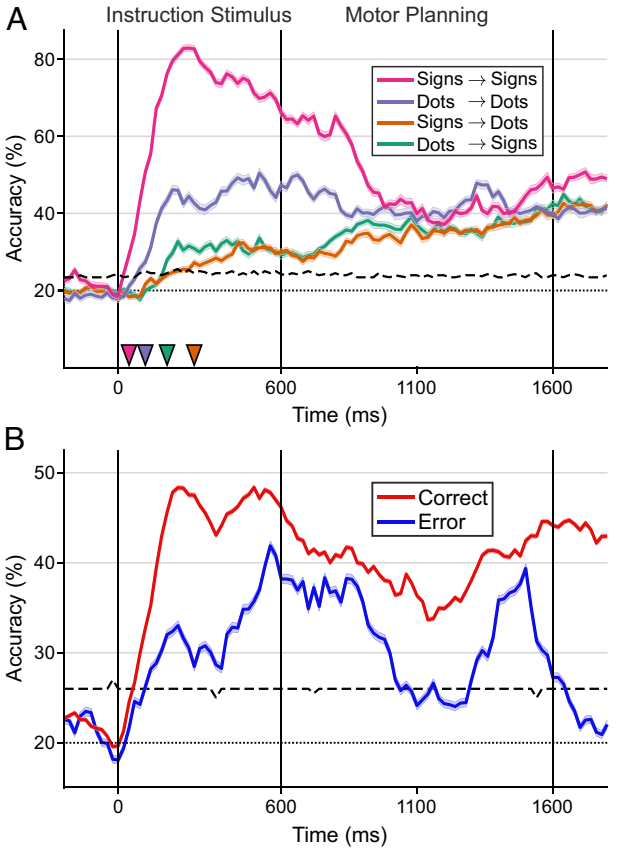

Fig. 5. Temporal dynamics of NCL population decoding. (*A*) Accuracy (% correct) of linear SVM classifiers trained and tested throughout progression of a trial (see *Methods* for details). Colored lines show mean and shaded error bars the SEM over resamples for each of four specific within- and across-protocol conditions (color-coded). Vertical solid lines indicate task periods, the vertical dashed line depicts shuffled label classifier performance (95th percentile, mean over four conditions). The colored markers show the time of first above-chance classification accuracy for each condition, lines stayed above chance level after these time points. (*B*) The accuracy (% correct) of linear SVM classifiers was trained on the activity of correct trials pooled over stimulus protocol and tested on either new correct trials (red line) or error trials (blue line). Layout of graph as in *A*.

significant decoding appeared also later after stimulus onset ($latency_{dot\text{-}sign}$ = 180 ms, $latency_{sign\text{-}dot}$ = 280 ms).

We further utilized this decoding approach to examine whether the neuronal population irrespective of number selectivity carried behaviorally relevant information. Analogous to the above, we trained an SVM classifier on correct trials pooled over all stimulus protocols in a time-resolved manner (n = 164 neurons; see *Methods* for further details). We then tested the trained model on activity from both new correct trials and from error trials. Classification accuracy for correct trials rose sharply after instruction stimulus onset and remained well above chance throughout stimulus and planning periods (Fig. 5*B*). For error trials, however, classification accuracy was worse compared to correct trials throughout the trial phases and temporarily dropped below chance. Particularly during instruction stimulus presentation, the accuracy of error trial prediction remained close to chance, indicating that already during the presentation of the instructing stimulus, the population of neurons erroneously encoded the instructed number and failed to associate signs with dot numerosities (Fig. 5*B*).

These analyses with all recorded neurons irrespective of number selectivity confirmed previous findings from the subpopulation of association neurons. First, as soon as the instructing stimulus is presented, the NCL extracted numerical values. Second, after a brief delay relative to stimulus onset, the NCL significantly associated numerical values across protocols. Third, instruction number representation within the NCL was more precise for the sign protocol. And last, NCL represented this information in a behaviorally relevant manner.

Discussion

We instructed crows to produce a specific number of self-generated pecks. As instruction stimuli, we not only used dot displays that allowed a direct judgment of the number of dots but also Arabic numeral signs that the crows had learned to associate with specific numerical values 1 to 5. Single-neuron recordings in NCL showed that half of the neurons were selectively encoding the numerical value of the instruction stimuli during their presentation. This is a higher proportion of number-selective neurons compared to previous publications (34–36) which may be due to slight differences in selection criteria to detect those neurons. Most of these neurons were tuned to the same preferred number in dot and sign protocols, i.e., these number association neurons linked the numerical values presented in dot displays to signs and in a behaviorally relevant manner. These association neurons, as well as the entire population of NCL neurons, encoded numerical values associated with signs with higher precision.

Associations in the NCL. Few studies so far have investigated the neuronal underpinnings of stimulus associations in the avian brain. In these studies, the NCL was demonstrated to contain neurons that selectively represent learned association between pairs of arbitrary, meaningless stimuli. When crows were trained to associate visual stimuli with visual stimuli, and auditory stimuli with visual stimuli, half of the recorded NCL neurons signal within and cross-modal association (45). Another set of studies demonstrated that such association neurons are gradually established while the crows learn to associate new pictures (47), but only a subset of dedicated NCL neurons seem to be enabled to form such associations (48).

The current study similarly required crows to form long-term associations through training. A special feature of our study is that not arbitrary pictures and shapes without inherent meaning, but an abstract numerical meaning, namely cardinal values that are rank-ordered among themselves, were associated with signs. Such semantic associations require not only memory function but also information about numerical quantity. The NCL shows these requirements as it is not only engaged in memory functions (50–52) but also constitutes a key area for numerical processing in the avian endbrain (32–38).

The described number association neurons form an ideal neuronal substrate for such semantic stimulus associations. Neuronal association signals emerged quickly after instruction stimulus presentation. This constitutes an efficient neuronal solution to map number information from different presentation formats onto the same numerical space. The neurons' failure to form such semantic associations resulted in a higher probability of the crow to make errors. This indicates that associative signals early during the stimulus presentation phase are necessary for the crows to decipher the correct instruction number from different stimulus formats. Of course, this neuronal representation can only explain a fraction of errors as the instruction stimulus provides only a first potential source of error, and other potential error sources accumulate during the trial progression. This associative neuronal signal during instruction stimulus presentation can later in the trial ease sensorimotor number transformation to give rise to number selective sensorimotor neurons in the crow telencephalon that signal the impending number of self-generated actions (33, 53).

Semantic Associations in the Avian NCL in Comparison to the Primate PFC. Comparable semantic number association neurons described here for the NCL of crows have only been reported in the PFC of the macaque monkey. Neurons in the primate PFC are known to readily associate arbitrary stimuli (54, 55). Diester and Nieder (27) trained monkeys in a delayed-match-to-sample task to discriminate the numerosity in dot displays and to match the numerical values associated with Arabic numeral shapes to numerosities 1 to 4. Single-neuron recordings showed 23% of association neurons in the monkey PFC (in contrast, only 2% in the intraparietal sulcus, which was concluded to play no role in this type of numerical association). Besides a similar fraction of association neurons in PFC and NCL, also the time course of association activity early in the stimulus period is comparable between PFC and NCL. Last, association neurons in the PFC tended to show more precise number representations for signs, just as we showed for the crow NCL. The close correspondence of the mechanisms of how the primate PFC and the corvid NCL establish semantic number association underlines the NCL's importance as the avian equivalent of the primate PFC both in the number domain (56) and for cognition control in general (57).

In the human brain, PFC neurons have not been probed for numerical associations. However, neuronal responses to numerosity in dot displays and to numerical values in Arabic numerals have recently been recorded in the medial temporal lobe (MTL) regions of human epilepsy patients performing calculation tasks (58). Instead of association neurons responding equally well to nonsymbolic number in dot displays and symbolic number in numerals, two separate populations of neurons were reported that either encoded nonsymbolic or symbolic numbers, but not both. Similar to our findings in the crow NCL, however, numerical representations encoded by the one population of MTL neurons in numerals lacked a numerical distance effect and tuning was more precise compared to numerosity representations in dot arras encoded by the other population of MTL neurons.

The comparison of crow (and monkey) data with human findings is of course not fully appropriate, as only humans are truly symbol-competent. However, the number association neurons in crows could point to a phylogenetic preadaptation of the brains of

cognitively advanced vertebrates being able to link visual shapes with numerical meaning. This associative capability might later have been exploited when humans evolved symbol understanding (8, 59). After all, the association of an arbitrary visual shape with a numerical value is one of the first steps when children learn to master a symbolic number system (5). We speculate that the neuronal correlates of semantic association we reported here in crows form a putative prerequisite for symbolic number representations.

Methods

Animals. Two hand-raised male carrion crows (*Corvus corone*) obtained from the institute's breeding facility were used. They were housed in spacious indoor aviaries (L x W x H: 3.6 x 2.4 x 3 m) in social groups of up to four individuals with daylight and a natural light-dark cycle under controlled temperature and air humidity conditions (for details, see ref. 60). The crows were kept on a controlled feeding protocol and earned food as a reward during training and recording periods. Additional food was supplemented after the daily sessions if necessary. Water was always provided ad libitum. All procedures were conducted according to the national guidelines for animal experimentation and approved by the national authority, the Regierungspräsidium Tübingen, Germany. Other parts of the current dataset were published in a previous publication (33).

Experimental Apparatus. Training and recording occurred in a darkened operant conditioning chamber. The crows were loosely strapped to a wooden perch using leather jesses and placed in front of a 15" touchscreen monitor (3M MicroTouch; 60 Hz refresh rate). A light barrier, consisting of an infrared light emitter/detector fixed on the ceiling of the chamber and a reflector foil attached to the crow's head, was used to ensure the crows maintained a central head position in front of the monitor (viewing distance: 14 cm). A custom-built automated feeder for reward delivery was positioned below the monitor. Birdseed pellets (Beo Special, Vitakraft) and mealworms (*Tenebrio molitor* larvae) were used as rewards. Loudspeakers (Visaton WB10) for auditory feedback, as well as an infrared camera (Genius iSlim 321R) for observational control, were also installed in the chamber. Presentation of stimuli and collection of behavioral responses was managed by the CORTEX system (National Institute for Mental Health, Bethesda, MD). Electrophysiological data were recorded using a PLEXON MAP system (Plexon Inc., Dallas, TX).

Behavioral Protocol. The crows were trained on a computerized task to plan and produce a visually instructed number of pecking responses. A ready cue (small white circle in the center of the touchscreen) indicated to the crow that a trial could be initiated. To initiate a trial, the crow had to position its head centrally in front of the monitor, thereby closing an infrared light barrier. Moving out of this predefined position before the start of the motor execution period terminated the ongoing trial. After the initiation of a trial, an empty gray background circle (size: 26.1° of visual angle) was displayed for the duration of the baseline period (300 ms). Next, an instruction stimulus (600 ms) cued the number of 1 to 5 pecking actions to produce. This impending number of actions had to be maintained in working memory throughout the following motor planning period (1,000 ms). The appearance of a second, smaller gray circle (confirmation stimulus, or "enter key"; size: 11.4° of visual angle) below the empty background circle (now serving as enumeration stimulus) marked the end of the motor planning period and the beginning of the motor execution period. In this motor execution period, the crow had to sequentially produce the cued number of pecks in a predefined way: the crow had to produce each unitary response by pecking at the enumeration stimulus within 600 ms of its displaying onset. The enumeration stimulus disappeared after each peck, followed by a short and systematically varied interresponse interval after which the enumeration stimulus would reappear for as often as the crow would continue to add more pecks. The temporal arrangements of the motor execution period, as well as controls for timing of responses, have been described in detail before (33).

The crow signaled it produced the instructed number of responses by pecking at the confirmation stimulus (enter key). Both types of pecking responses (to the enumeration stimulus and the confirmation stimulus) were accompanied by specific sounds (250 ms duration) serving as auditory feedback for registered responses. A trial was counted correct if the number of pecks produced by the crow prior to the confirmation response matched the instructed number. Correct trials triggered dispensary of a food reward accompanied by a reward tone. If the crow gave a premature confirmation response (e.g., $n-1$, with n as the instructed number) or exceeded the requested number of enumeration responses by one ($n+1$), an error was detected. If the crow exited the light barrier before the onset of the response period, reacted prematurely during the waiting interval, missed the pecking time interval, or missed the monitor location of the enumeration or confirmation stimuli, the trial was aborted but not counted as error. All errors and trial abortions resulted in the withholding of reward accompanied by a specific sound, a visual feedback signal, and a brief timeout period, in which initiation of the next trial was delayed.

We used two numerical presentation protocols with a standard and control condition for each numerical value ranging from 1 to 5, as described below. The numerical values, protocols, and conditions were presented in a pseudorandomized and balanced order.

Stimuli. Two different numerical presentation protocols with numerical values 1 to 5 as instruction stimuli were used: The dot protocol showed a numerosity dot display with 1 to 5 black dots; the sign protocol consisted of five different visual shapes (Arabic numerals) that the crows had learned to associate as signs with the instructed number of actions. Both dot and sign displays were shown on a gray circular background.

For both protocols we used two stimulus conditions (standard and control), thereby controlling for non-numerical factors. For the dot protocol, the different stimulus conditions controlled for low-level visual features (total dot area and dot density) that covary with numerosity. In the standard condition, dot displays consisted of 1 to 5 dots of pseudorandomized size (1.2 to 5.5° of visual angle) presented at pseudorandom locations on the gray background circle, with the only requirement that dots were not overlapping or touching. In the control condition, total dot area and density were kept constant across numerical values.

For the sign protocol, black Arabic numerals 1 to 5 of pseudorandom size (15 to 26 pts., 2.9 to 4.9° of visual angle) were placed at a pseudorandom location on the background. "Arial" was used as the standard font-type, whereas "Times New Roman," "Souvenir," and "Lithograph Light" were used as control fonts. To prevent the animal from memorizing or rote learning individual stimuli, 5 complete sets of stimuli for every combination of protocol, condition, and numerosity were generated anew before each session using MATLAB (Version R2020b, MathWorks Inc., Natick, MA).

Surgery and Recordings. After crows reached the learning criterion (described in detail in ref. 33), we implanted custom-made microdrives carrying electrodes for electrophysiological recordings. All surgeries were performed while the animals were under general ketamine/xylazine anesthesia. The head was placed in the stereotaxic holder that was customized for crows with the anterior fixation point (that is, beak bar) at 45° angle below the horizontal axis of the instrument. Using stereotaxic coordinates (center of craniotomy: anterior–posterior +5 mm relative to interaural point as zero; medial–lateral 13 mm relative to midline), we chronically implanted two microdrives with four electrodes each in the left or right hemispheres, a connector for the head stage and a small head post to hold the reflector for the light barrier. Glass-coated tungsten microelectrodes with 2 MΩ impedance (Alpha Omega) were used. The electrodes targeted the corvid NCL, which is characterized by dopaminergic cells and was histologically verified before (61, 62). Crows received analgesics after surgery (35).

Few days after surgery, when the crows had fully recovered, we recorded single-unit activity in the behaving crows. We recorded from both hemispheres of both crows (9 sessions from right NCL and 62 sessions from left NCL in crow 1; 5 sessions from left NCL and 51 sessions from right NCL for crow 2). Every session the birds were placed in the recording setup and a head stage containing an amplifier was plugged into the connector implanted on the bird's head and connected to a second amplifier/filter and the PLEXON MAP box outside of the setup by a cable above and behind the bird's head (all components by Plexon Inc., Dallas, TX). Each recording session started with advancing the electrodes until a proper neuronal signal was detected. Neurons were never preselected based on task responsiveness. PLEXON's Offline Sorter was used to manually offline sort spikes into single-unit waveforms.

Data Analysis. All data analyses were carried out using MATLAB (Version R2020b, MathWorks Inc., Natick, MA). Values reported in the main text refer and figures

refer to the mean ± SEM unless stated otherwise. SEM was calculated as the SD divided by the square root of the sample size.

Neuronal Tuning and Selectivity Analysis. We only included neurons in all following analyses that had an average firing rate of at least 0.5 Hz in a relevant task window (baseline period onset until motor planning period offset) and were recorded for at least two correct trials for each of 20 specific trial conditions (5 instruction numbers × 2 stimulus protocols × 2 stimulus conditions).

Neuronal activity during the instructing stimulus period was evaluated in a 900 ms time window from 100 ms prior to stimulus onset until 200 ms after stimulus offset. The analysis window thus reached 200 ms into the motor planning period but based on the neurons' response latency we only analyzed activity related to the stimulus presentation and visual offset. The mean visual latency for crow NCL neurons is 144 ms (42). Therefore, the neuronal activity relative to the physical task periods is delayed by this amount of time (i.e., 144 ms, on average). The activity of the first 200 ms of the motor planning period has not been previously reported or analyzed (cf. to ref. 33).

A two-factor sliding-window ANOVA (200 ms window, 10 ms step-size, $P < 0.05$) was performed in this 900 ms instructing stimulus period window. We assessed single-neuron selectivity to the task variables "number" (instruction numbers 1 to 5) and "protocol" (dots and signs). As stimulus condition (standard and control) differed for dot and sign protocols, it was not included as a factor into the ANOVAs. If there was a significant main effect for the number factor in more than 11 consecutive time-bins (at least 300 ms interval), this neuron and respective interval were categorized number-selective. Only the intervals containing the largest modulation in firing for different instruction numbers were used if there were multiple such selective intervals for a neuron.

For every number-selective neuron and both stimulus protocols, the instruction number eliciting the highest firing rate in the neuron's respective selective interval was termed the preferred numerical value. We constructed neuronal response functions by normalizing a neuron's average firing rate to its most- and least-preferred instruction number. The populations' response functions were yielded by averaging tuning function of all number-selective neurons preferring each individual numerical value in each stimulus protocol. The populations' average tuning functions were also expressed as a function of absolute numerical distance. Pairs of numerical distances were statistically compared using Wilcoxon signed-rank tests.

Correlation Analysis. A correlation analysis was used to compare the tuning of individual neurons between both stimulus protocols, that is, dots and signs. The following steps were performed for each number-selective neuron in sliding window fashion (200 ms windows with 10 ms steps, from 400 ms prior to instructing stimulus onset until 300 ms after stimulus offset). First, for each cell and in each time-bin, we sampled 4 trials per instruction number and stimulus protocol at random (4 trials x 5 instruction number x 2 stimulus protocols, amounting to 40 sampled trials). Second, we constructed tuning curves from the sampled trials by averaging firing rate in the 200 ms time window over trials of the five instruction numbers, separately for the dot and sign protocol. Third, the cross-correlation coefficient (CC) from these tuning functions was calculated according to the following formulae:

$$\mathrm{CC} = \frac{\sum_{n=1}^{5} (t_{dot}(n) - \bar{t}_{dot})(t_{sign}(n) - \bar{t}_{sign})}{\sqrt{\sum_{n=1}^{5} (t_{dot}(n) - \bar{t}_{dot})^2} \sqrt{\sum_{n=1}^{5} (t_{sign}(n) - \bar{t}_{sign})^2}}, \qquad [\mathbf{1}]$$

$$\bar{t}_{dot} = \frac{1}{5} \sum_{n=1}^{5} t_{dot}(n), \qquad [\mathbf{2}]$$

$$\bar{t}_{sign} = \frac{1}{5} \sum_{n=1}^{5} t_{sign}(n), \qquad [\mathbf{3}]$$

where n are the instruction numbers between 1 and 5, and $t_{dot}(n)$ and $t_{sign}(n)$ are the tuning functions for the dot and the sign protocol, respectively. The CC ranges between 1 for perfect correlation and −1 for perfect anticorrelation and is 0 when there is no correlation. To compare CCs yielded in such way to CCs expected by chance (called shuffled predictor, or SP, values), we shuffled instruction number labels for each trial sampled in the first step, thus eliminating the relationship between a cell's firing and the instruction number. We then constructed dummy tuning curves according to the second step and calculated SP values from those as in the third step. We repeated the above steps 1,000 times, each time with a different set of randomly drawn trials. Thus, we ended up with distributions of 1,000 CCs and SPs for each cell in each time-bin.

To quantify the similarity in the cell's tuning between both stimulus protocols compared to random tuning due to chance, we calculated ROC with distributions of CC and SP values. The ROC measures the separability of two distributions with the AUROC curve summarizing how well these distributions are separated. An AUROC value of 0.5 indicates largely overlapping distributions and, in this instance, would mean that the tuning of a given cell at a given time point is as similar between stimulus protocols as expected by chance. On the other end, an AUROC value of 1 indicates perfectly separated distributions, and here, would indicate identical tuning to numerical values of dots and signs for a given cell at a given point in time. We used the CCs as reference distributions for calculating the AUROCs. We determined a threshold for significance as the mean AUROC during the baseline period plus 3 times its SD. Any time-bin's AUROC value exceeding this threshold was indicating a cross-correlation significantly above chance, and any neuron with such significant time windows was further termed "association neuron".

Error Trial Analyses. To investigate whether failure to properly associate signs with their numerical value influences the behavioral success of a trial, we adapted the above cross-correlation analysis to error trials, in which the crows were producing an incorrect number of enumeration pecks. Similar to above, we calculated CCs for all association neurons in a time-resolved manner (identical to above sliding window parameters) between tuning curves of correct trials in the dot protocol and tuning curves yielded from error trials in the sign protocol. Since the crows produced few errors, particularly for instruction number 1, tuning curves were constructed only for instruction numbers with recorded error trials (but at least two instruction numbers). These error CCs were compared to CCs calculated from correct trials from both stimulus protocols, restricted to the same instruction numbers.

Time-Resolved Classifier Analyses. We performed time-resolved classification analyses within and across stimulus protocols using linear multi-class SVM classifier models (63). For this, we considered only neurons that were recorded for at least 10 correct trials per class, i.e., instruction number, in both stimulus protocols (that is, 10 trials x 5 instruction numbers x 2 stimulus protocols, at least 100 recorded trials). We used a sliding window (200 ms length, 20 ms step size, from baseline onset until 300 ms after motor planning offset) and trained and tested multiple SVM models in each of these windows. In each such window, we trained models on normalized, average firing rates (z-scoring parameters yielded from the training subset) in either dot or sign trials, used one-to-one classification to deal with 5 classes, and followed a scheme similar to a 10-fold cross-validation: Nine trials per class of one protocol were used for training and one trial per class of either the same protocol (within protocol), or the respective other protocol (across protocol) were then used for testing the SVM models per split. This was repeated 10 times, each time with another split of trials for training and testing. The number of correct classifications (labels predicted by the model equals the true label) divided by the number of overall classifications over all 10 cross-validation folds yields an accuracy measure of classifier performance. Accordingly, we calculated one accuracy measure for each specific condition (two within protocol conditions, i.e., training and testing on trials of the same stimulus protocol, and two cross-protocol conditions) per time-bin. We repeated this procedure 50 times, each time with a new subset of randomly drawn trials for each neuron. To assess chance level classifier performance for each of the four specific conditions, we repeated the above procedure (including 10-fold cross-validation and z-scoring) with permuted trial labels, shuffling 20 times per resample (50 resamples × 20 shuffles = 1,000 reshuffles for chance level accuracy distribution).

We also trained SVM classifier models on correct trials pooled over stimulus protocol and tested these models on the activity of previously unseen correct, and error trials. As this procedure is identical to the above, we only describe deviating aspects in the following. We only considered neurons that had at least one error trial per instruction number. This number was small because there were very few incorrect trials for the numerical value 1. Nine correct trials per class were used for training, and either one correct or one incorrect trial per class was then used for testing the SVM models per split. Again, this was repeated 10 times, each time

with another split of trials. We resampled trials 1,000 times. All other procedures for this classifier were identical to the analyses above. We thus receive two time-resolved accuracy measures from this analysis: one for the autoclassification of correct trials and one for the prediction of incorrect trial labels from models trained on firing rates of correct trials.

Data, Materials, and Software Availability. All study data are included in the main text.

ACKNOWLEDGMENTS. This work was supported by a DFG grant NI 618/12-1 to A.N.

1. A. Nieder, The adaptive value of numerical competence. *Trends Ecol. Evol.* **35**, 605–617 (2020).
2. A. Nieder, *A Brain for Numbers: The Biology of the Number Instinct* (MIT Press, 2019).
3. M. Piazza, Neurocognitive start-up tools for symbolic number representations. *Trends Cogn. Sci.* **14**, 542–551 (2010).
4. S. Dehaene, F. Al Roumi, Y. Lakretz, S. Planton, M. Sablé-Meyer, Symbols and mental programs: A hypothesis about human singularity. *Trends Cogn. Sci.* **26**, 751–766 (2022).
5. H. Wiese, Iconic and non-iconic stages in number development: The role of language. *Trends Cogn. Sci.* **7**, 385–390 (2003).
6. G. Dehaene-Lambertz, E. S. Spelke, The infancy of the human brain. *Neuron* **88**, 93–109 (2015).
7. S. Carey, D. Barner, Ontogenetic origins of human integer representations. *Trends Cogn. Sci.* **23**, 823–835 (2019).
8. A. Nieder, Prefrontal cortex and the evolution of symbolic reference. *Curr. Opin. Neurobiol.* **19**, 99–108 (2009).
9. T. Matsuzawa, Use of numbers by a chimpanzee. *Nature* **315**, 57–59 (1985).
10. S. T. Boysen, G. G. Berntson, Numerical competence in a chimpanzee (Pan troglodytes). *J. Comp. Psychol.* **103**, 23–31 (1989).
11. D. A. Washburn, D. M. Rumbaugh, Ordinal judgments of numerical symbols by macaques (Macaca mulatta). *Psychol. Sci.* **2**, 190–193 (1991).
12. I. Diester, A. Nieder, Numerical values leave a semantic imprint on associated signs in monkeys. *J. Cogn. Neurosci.* **22**, 174–183 (2010).
13. D. Biro, T. Matsuzawa, Numerical ordering in a chimpanzee (Pan troglodytes): Planning, executing, and monitoring. *J. Comp. Psychol.* **113**, 178–185 (1999).
14. D. Biro, T. Matsuzawa, Use of numerical symbols by the chimpanzee (Pan troglodytes): Cardinals, ordinals, and the introduction of zero. *Anim. Cogn.* **4**, 193–199 (2001).
15. K. Murofushi, Numerical matching behavior by a chimpanzee (Pan troglodytes): Subitizing and analogue magnitude estimation. *Jpn. Psychol. Res.* **39**, 140–153 (1997).
16. M. J. Beran, D. M. Rumbaugh, E. S. Savage-Rumbaugh, Chimpanzee (Pan troglodytes) counting in a computerized testing paradigm. *Psychol. Rec.* **48**, 3–19 (1998).
17. M. J. Beran, Long-term retention of the differential values of Arabic numerals by chimpanzees (Pan troglodytes). *Anim. Cogn.* **7**, 86–92 (2004).
18. L. Xia, J. Emmerton, M. Siemann, J. D. Delius, Pigeons (Columba livia) learn to link numerosities with symbols. *J. Comp. Psychol.* **115**, 83–91 (2001).
19. A. Olthof, W. A. Roberts, Summation of symbols by pigeons (Columba livia): The importance of number and mass of reward items. *J. Comp. Psychol.* **114**, 158–166 (2000).
20. I. M. Pepperberg, Evidence for conceptual quantitative abilities in the African grey parrot: Labeling of cardinal sets. *Ethology* **75**, 37–61 (1987).
21. I. M. Pepperberg, S. Carey, Grey parrot number acquisition: The inference of cardinal value from ordinal position on the numeral list. *Cognition* **125**, 219–232 (2012).
22. S. R. Howard, A. Avarguès-Weber, J. E. Garcia, A. D. Greentree, A. G. Dyer, Symbolic representation of numerosity by honeybees (Apis mellifera): Matching characters to small quantities. *Proc. R. Soc. B Biol. Sci.* **286**, 20190238 (2019).
23. D. A. Washburn, Stroop-like effects for monkeys and humans: Processing speed or strength of association? *Psychol. Sci.* **5**, 375–379 (1994).
24. S. T. Boysen, G. G. Berntson, Responses to quantity: Perceptual versus cognitive mechanisms in chimpanzees (Pan troglodytes). *J. Exp. Psychol. Anim. Behav. Process.* **21**, 82–86 (1995).
25. V. Schmitt, J. Fischer, Representational format determines numerical competence in monkeys. *Nat. Commun.* **2**, 257 (2011).
26. S. M. Carlson, A. C. Davis, J. G. Leach, Less is more: Executive function and symbolic representation in preschool children. *Psychol. Sci.* **16**, 609–616 (2005).
27. I. Diester, A. Nieder, Semantic associations between signs and numerical categories in the prefrontal cortex. *PLoS Biol.* **5**, 2684–2695 (2007).
28. E. D. Jarvis *et al.*, Avian brains and a new understanding of vertebrate brain evolution. *Nat. Rev. Neurosci.* **6**, 151–159 (2005).
29. S. D. Briscoe, C. W. Ragsdale, Evolution of the chordate telencephalon. *Curr. Biol.* **29**, R647–R662 (2019).
30. G. F. Striedter, R. G. Northcutt *Brains Through Time: A Natural History of Vertebrates* (Oxford University Press, 2019), 10.1093/oso/9780195125689.001.0001.
31. H. M. Ditz, A. Nieder, Numerosity representations in crows obey the Weber-Fechner law. *Proc. R. Soc. B Biol. Sci.* **283**, 20160083 (2016).
32. M. E. Kirschhock, H. M. Ditz, A. Nieder, Behavioral and neuronal representation of numerosity zero in the crow. *J. Neurosci.* **41**, 4889–4896 (2021).
33. M. E. Kirschhock, A. Nieder, Number selective sensorimotor neurons in the crow translate perceived numerosity into number of actions. *Nat. Commun.* **13**, 6913 (2022).
34. H. M. Ditz, A. Nieder, Neurons selective to the number of visual items in the corvid songbird endbrain. *Proc. Natl. Acad. Sci. U.S.A.* **112**, 7827–7832 (2015).
35. H. M. Ditz, A. Nieder, Sensory and working memory representations of small and large numerosities in the crow endbrain. *J. Neurosci.* **36**, 12044–12052 (2016).
36. H. M. Ditz, A. Nieder, Format-dependent and format-independent representation of sequential and simultaneous numerosity in the crow endbrain. *Nat. Commun.* **11**, 1–10 (2020).
37. L. Wagener, M. Loconsole, H. M. Ditz, A. Nieder, Neurons in the endbrain of numerically naive crows spontaneously encode visual numerosity. *Curr. Biol.* **28**, 1090–1094 (2018).
38. D. Kobylkov, U. Mayer, M. Zanon, G. Vallortigara, Number neurons in the nidopallium of young domestic chicks. *Proc. Natl. Acad. Sci. U.S.A.* **119**, e2201039119 (2022).
39. A. Nieder, Inside the corvid brain–Probing the physiology of cognition in crows. *Curr. Opin. Behav. Sci.* **16**, 8–14 (2017).
40. O. Güntürkün, The avian "prefrontal cortex" and cognition. *Curr. Opin. Neurobiol.* **15**, 686–693 (2005).
41. D. Lengersdorf, M. C. Stüttgen, M. Uengoer, O. Güntürkün, Transient inactivation of the pigeon hippocampus or the nidopallium caudolaterale during extinction learning impairs extinction retrieval in an appetitive conditioning paradigm. *Behav. Brain Res.* **265**, 93–100 (2014).
42. L. Veit, K. Hartmann, A. Nieder, Neuronal correlates of visual working memory in the corvid endbrain. *J. Neurosci.* **34**, 7778–7786 (2014).
43. M. Johnston, B. Porter, M. Colombo, Delay activity in pigeon nidopallium caudolaterale during a variable-delay memory task. *Behav. Neurosci.* **133**, 563–568 (2019).
44. P. Rinnert, A. Nieder, Neural code of motor planning and execution during goal-directed movements in crows. *J. Neurosci.* **41**, 4060–4072 (2021).
45. F. W. Moll, A. Nieder, Modality-invariant audio-visual association coding in crow endbrain neurons. *Neurobiol. Learn. Mem.* **137**, 65–76 (2017).
46. F. W. Moll, A. Nieder, Cross-modal associative mnemonic signals in crow endbrain neurons. *Curr. Biol.* **25**, 2196–2201 (2015).
47. L. Veit, G. Pidpruzhnykova, A. Nieder, Associative learning rapidly establishes neuronal representations of upcoming behavioral choices in crows. *Proc. Natl. Acad. Sci. U.S.A.* **112**, 15208–15213 (2015).
48. L. Veit, G. Pidpruzhnykova, A. Nieder, Learning recruits neurons representing previously established associations in the corvid endbrain. *J. Cogn. Neurosci.* **29**, 1712–1724 (2017).
49. M. E. Kirschhock, A. Nieder, Numerical representation for action in crows obeys the Weber-Fechner law. *Psychol. Sci.* (2023), in press.
50. P. Rinnert, M. E. Kirschhock, A. Nieder, Neuronal correlates of spatial working memory in the endbrain of crows. *Curr. Biol.* **29**, 2616–2624 (2019).
51. A. Nieder, L. Wagener, P. Rinnert, A neural correlate of sensory consciousness in a corvid bird. *Science* **369**, 1626–1629 (2020).
52. L. Wagener, A. Nieder, Categorical representation of abstract spatial magnitudes in the executive telencephalon of crows. *Curr. Biol.* **33**, 2151–2162.e5 (2023).
53. G. Anobile, R. Arrighi, E. Castaldi, D. C. Burr, A sensorimotor numerosity system. *Trends Cogn. Sci.* **25**, 24–36 (2021).
54. G. Rainer, S. C. Rao, E. K. Miller, Prospective coding for objects in primate prefrontal cortex. *J. Neurosci.* **19**, 5493–5505 (1999).
55. J. M. Fuster, M. Bodner, J. K. Kroger, Cross-modal and cross-temporal association in neurons of frontal cortex. *Nature* **405**, 347–351 (2000).
56. A. Nieder, The evolutionary history of brains for numbers. *Trends Cogn. Sci.* **25**, 608–621 (2021).
57. A. Nieder, Neuroscience of cognitive control in crows. *Trends Neurosci.* **46**, 783–785 (2023), 10.1016/j.tins.2023.07.002.
58. E. F. Kutter, J. Bostroem, C. E. Elger, F. Mormann, A. Nieder, Single neurons in the human brain encode numbers. *Neuron* **100**, 753–761 (2018).
59. A. Nieder, Neural constraints on human number concepts. *Curr. Opin. Neurobiol.* **60**, 28–36 (2020).
60. A. Hoffmann, V. Rüttler, A. Nieder, Ontogeny of object permanence and object tracking in the carrion crow, Corvus corone. *Anim. Behav.* **82**, 359–367 (2011).
61. L. Veit, A. Nieder, Abstract rule neurons in the endbrain support intelligent behaviour in corvid songbirds. *Nat. Commun.* **4**, 1–11 (2013).
62. Y. Kersten, B. Friedrich-Müller, A. Nieder, A brain atlas of the carrion crow (Corvus corone). *J. Comp. Neurol.* **530**, 3011–3038 (2022).
63. C. C. Chang, C. J. Lin, LIBSVM: A Library for support vector machines. *ACM Trans. Intell. Syst. Technol.* **2**, 1–27 (2011).